Journal of New Technology and Materials (JNTM)
J. New Technol. Mater.
Vol. 10, N°01 (2020)69-74

OEB Univ. Publish. Co.

# Microstructural and mechanical behaviour of spray formed Al-Si-Gr composites synthesised by friction stir processing

Abhijeet Bajpai[a]*, Dhruv Singh Baghel[a], Raj Kumar Singh[a] and Pradeep Kumar Yadav[b]

[a]*Department of Mechanical Engineering, Rewa Engineering College, Rewa, Madhya Pradesh, India, 486001*
[b]*Maulana Azad National Institute of Technology, Bhopal, Madhya Pradesh, India, 462003*
*Corresponding author, email: bhaiyuabhijeet@gmail.com

Received date: Dec. 24, 2019; revised date: May 28, 2020; accepted date: May 28, 2020

***Abstract***

*In this study, Al-Si-Gr composites for cylinder liner application were synthesised using a spray forming technique, aiming at improving the wear resistance. Silicon (Si) and graphite (Gr) particles, which do not distribute uniformly in the aluminium matrix by conventional processes, are dispersed uniformly throughout the composite using spray forming. Al–6Si-5Gr, Al-12Si-5Gr, and Al–18Si-5Gr composites were used to make disc-shaped spray form castings, and then their microstructures were studied. In spray form castings, it was found that the Si and Gr particles were distributed homogeneously in the Al-matrix. Friction stir processing (FSP) was performed on spray formed Al-Si-Gr composites. In the present work, FSP was introduced to refine the microstructure of spray formed Al-Si-Gr composites. The microstructure of the stir zone (SZ) was observed to be highly refined compared to the spray forming material. FSP resulted in the elimination of casting defects, especially porosity and complete homogenisation. Other than this FSPed sample showed higher hardness compared to spray formed sample.*

*Keywords: Spray forming; Friction stir processing; Al-Si-Gr composite; Microstructural refinement*

## 1. Introduction

Spray casting route has been extensively used to make preforms with equiaxed, cellular, and fine-grained microstructure. Although, a preform cast using spray deposition technique has poor mechanical properties with high porosity [1-2]. To prepare dense sheets of metal with excellent microstructural and mechanical properties, the porous casting must be deformed plastically and densified. Hot pressing, rolling, extrusion is some of the effective methods used to eliminate porosity and attain the required microstructural and mechanical properties [3-5]. However, recently Mishra et al. [6] developed FSP as a generic tool for microstructural modification. FSP diminishes the pores and brings the microstructural refinement. The most important objective of FSP in spray deposited material is to minimise porosity. Hosseinzadeh and Yapici [7] found that the hardness of Al2024-SiC composite produced by friction stir processing is higher than the as-received condition. However, as-received condition, composite exhibited better yield strength. Khodabakhshi et al. [8] concluded that the mechanical properties and microstructural features of the coating layer (aluminium alloy AA7075) on the surface of magnesium AZ31B alloy are improved after friction stir processing modification. Literature survey revealed that no research work had been done on the effect of friction stir processing (FSP) on the microstructural and mechanical behaviour of Spray Formed Al-Si-Gr composites.

The aim of the present research was to examine the effect of friction stir processing on the microstructural and mechanical behaviour of spray formed different Al-Si-Gr composites and its base alloys.

## 2. Materials and Methods

### *2.1. Materials preparation*

A schematic scratch of spray forming set-up is exhibited in Figure 1 [9]. The Al-Si alloys used in the present work were Al-6Si, Al-12Si & Al-18Si. The chemical compositions of the base alloys are shown in Table 1. An induction furnace was used to superheat the alloy 150°C above its melting temperature in a graphite crucible. Graphite particles with average size ~ 40μm and volume fraction 5wt% were reinforced in all three compositions during atomisation. Nitrogen gas was used for gas atomisation before the flow of the melt. The gas atomisation was done at a nitrogen gas pressure of 7 bar before melt flow. The metal droplets are sprayed and deposited on a substrate made of copper. The substrate was centred along the vertical axis of the atomiser. The distance of 35 cm was maintained between the nozzle opening and copper substrate to produce a disc shape preform for each experiment conducted for this study. The preform solidified over the copper substrate was taken out, and then specimens were cut near the central near-bottom region of each sample as shown in Figure 2.

Friction Stir Processing was performed at the traversed speed of 50 mm/min at 1025 rpm, and tilt angle was 2°.

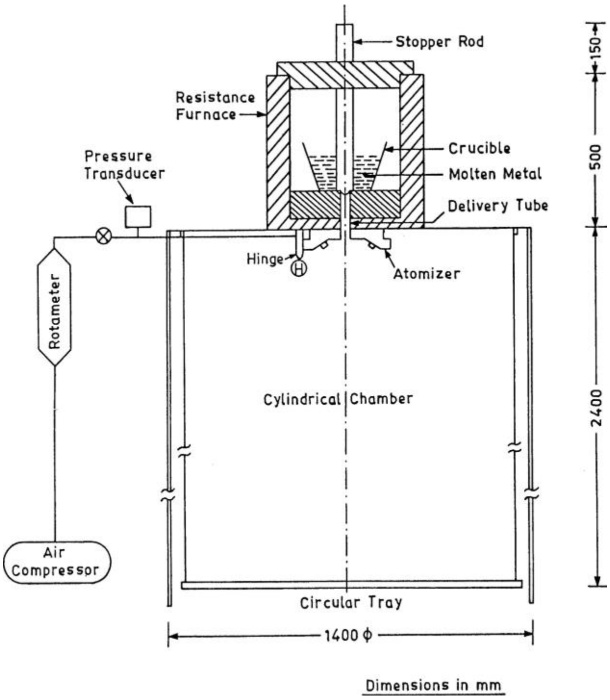


Figure 1. Schematic sketch of spray forming set-up [9]

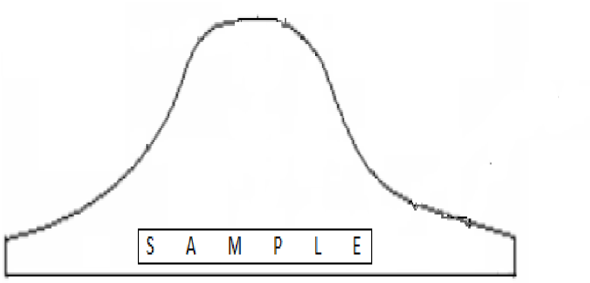


Figure 2. Spray deposit's shape collected over the substrate

*2.2. Density and hardness measurement*

The density of alloy and composites was by Archimedes principle. The hardness tests were performed using a Brinell-cum-Vicker's hardness tester (HPO 250, Heckert, Germany) at 10 N load. The diamond-shaped indentation was done at four different regions of each specimen. The average value of the three measurements was taken and reported in this paper.

*2.3. Tensile Tests*

The tensile test was performed on a universal testing machine (Model: H25KS, Tinius Olsen India Pvt Ltd., Noida, India) with 0.5 mm/minute strain rate of pulling specimen. The tensile test was done at all compositions, before and after FSP. The three measurements of the ultimate tensile strength (UTS), yield strength (0.2% proof strength), and percentage elongation (ductility) were recorded, and an average value reported.

Table 1: The chemical composition of test materials

| | Constituent elements (wt.%) | | | | | | |
|---|---|---|---|---|---|---|---|
| | Si | Mn | Mg | Cu | Fe | Ni | Al |
| LM13 alloy | 12 | 0.5 | 0.8 | 4.5 | 1 | 0.1 | Balance |
| LM25 alloy | 7.5 | 0.5 | 0.5 | 0.2 | 0.5 | 0.1 | Balance |
| LM30 alloy | 17.5 | 0.5 | 0.6 | 4.5 | 1 | 0.1 | Balance |

Table 2: Physical properties of composites

| | Theoretical Density (kg/m3) | Actual Density (kg/m3) | Porosity (%) |
|---|---|---|---|
| Al-18Si-5Gr (SF) | 2611.52 | 2171.51 | 16.85 |
| Al-12Si-5Gr (SF) | 2633.78 | 2205.72 | 16.25 |
| Al-6Si-5Gr (SF) | 2656.04 | 2238.16 | 15.73 |
| Al-18Si-5Gr (FSP) | 2611.52 | 2444.28 | 6.4 |
| Al-12Si-5Gr (FSP) | 2633.78 | 2474.01 | 6.06 |
| Al-6Si-5Gr (FSP) | 2656.04 | 2501.84 | 5.8 |

*2.4 Microstructural studies*

Specimens were cut down from the central near-bottom region of the preform, as shown in Figure 2 for its microstructural study. Standard metallographic practices were used to polish these samples. Keller's reagent was used to etch these samples. Microstructural studies of the specimens before and after the FSP were examined with a scanning electron microscope (SEM) (LEO 435 VP, Carl Zeiss Microscopy Gmbh, Germany) and X-Ray Diffrectometer (XRD) (D8 Advance, Bruker, Germany). In XRD analysis, the scanning speed was 0.02° 2θ /sec in the angular range of 20° to 120° (2θ).

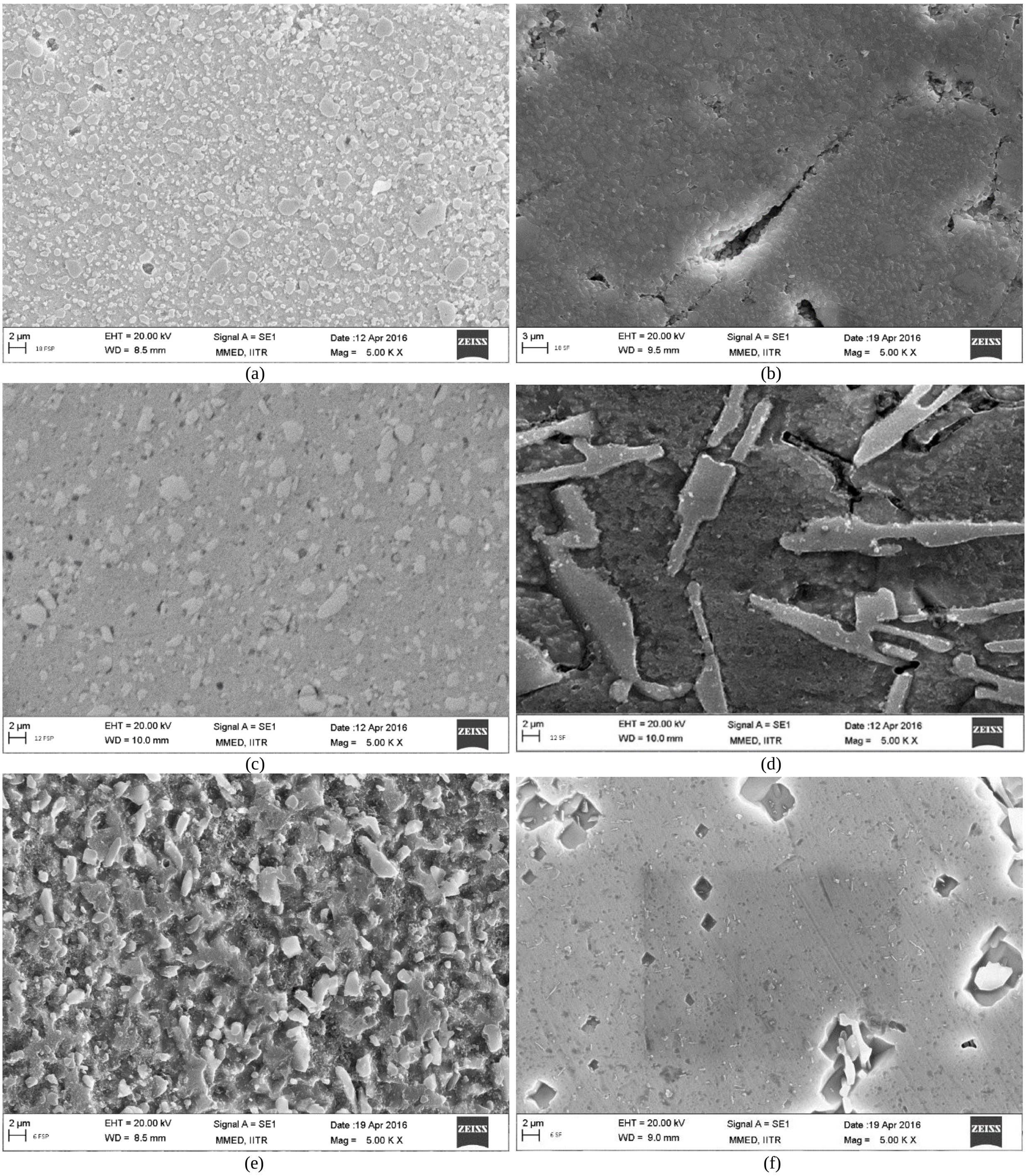


Figure 3. FESEM Micrographs of (a) Al-18Si-5Gr FSPed (b) Al-18Si-5Gr spray formed (c) Al-12Si-5Gr FSPed (d) Al-12Si-5Gr spray formed (e) Al-6Si-5Gr FSPed (f) Al-6Si-5Gr spray formed

Table 3: Mechanical properties of composites

| | Hardness (VHN) | UTS (MPa) | 0.2% Proof stress (MPa) | Ductility at UTS (%) |
|---|---|---|---|---|
| Al-18Si-5Gr (SF) | 52.2±1.1 | 67.42±3.04 | 39.42±1.32 | 2.68±0.13 |
| Al-12Si-5Gr (SF) | 46.3±0.9 | 82.43±4.32 | 38.04±1.21 | 5.32±0.38 |
| Al-6Si-5Gr (SF) | 41.5±0.7 | 62.71±2.78 | 23.09±1.65 | 7.14±0.67 |
| Al-18Si-5Gr (FSP) | 73.9±2.0 | 123.02±7.61 | 42.74±2.01 | 7.82±0.71 |
| Al-12Si-5Gr (FSP) | 66.1±1.5 | 142.35±8.82 | 41.54±2.17 | 11.71±0.82 |
| Al-6Si-5Gr (FSP) | 58.6±1.4 | 104.42±6.67 | 27.87±1.76 | 14.01±0.87 |

## 3. Results and Discussion

### *3.1. Microstructure*

In Figure 3, primary silicon can be seen in hyper-eutectic (Al-18Si-5Gr) composite as small spherical particles suspended homogeneously in Al-matrix in high contrast grey colour compared to eutectic silicon. Graphite particles are too small to be seen in this resolution. Silicon is soluble in aluminium in a liquid state. No macro-segregation of silicon is observed in the composite microstructure. Cooling of liquid takes place during their flight in the gas stream. Some droplets fully solidify some partially, and other remains in a liquid state before deposition on the copper substrate to form the spray deposited Al-Si-Gr composite. In this way, Spray forming produces fine-scale microstructure, which is refined and equiaxed. Spray generates micron size droplets. Rapid solidification effects in spray forming provided a significant microstructural and chemical homogeneity along with the refinement of second phase particle size and grains. High interfacial free energy between the two-component phases resulted in divorced morphology of the eutectic phase (Figure 3(d)). The average grain size found in the spray formed samples is 25-45 μm, whereas the grain size of primary silicon in the hyper-eutectic alloy was found to be of 5-15 μm. Equiaxed grains of primary aluminium was found, and silicon was present along the grain boundary and within these grains. With the increase in silicon content in the composite, we see that more primary silicon is present in the grain boundary.

Figure 3 shows higher magnification FESEM micrographs for different compositions of spray formed material and changes produced in it by FSP. We see there is no presence of primary silicon in Al-6Si-5Gr and Al-12Si-5Gr because of the less concentration of silicon than a eutectic point. In the case hypereutectic Al-18Si-5Gr, FESEM micrographs clearly show the presence of eutectic silicon and primary silicon phases in the composite. In these images, we majorly see a grey portion, which is the aluminium matrix. The white region is a silicon phase. The black region shows porosity and graphite particles. The size of primary silicon was found to be larger than eutectic silicon in the hypereutectic case, and the size of eutectic silicon in the hypereutectic case was found to be larger than eutectic and hypoeutectic Al-Si alloy compositions. During spray forming semi-liquid or semi-solid metal mass was continuously deposited and solidified on the copper substrate deposition surface. Rapid heat transfer takes place between this continuously depositing composite mass to the surroundings having high-speed atomising air velocity, and also to the already deposited composite on the substrate. Convection by the high-speed atomising air velocity and conduction by previously deposited mass leads to a high rate of heat transfer. Therefore, the high rate of heat transfers from the melt and the formation of nuclei in the composite leads to faster solidification of spray deposited composite and thereby formed equiaxed structure. Particulate form of the silicon in the structure of composite indicates rapid solidification of the deposit [10-12]. The FSP's rotating tool generates frictional heat and stirs the composite. As a result, there is a proper homogenisation of the matrix [13].

Figure 3b shows the spray formed Al-18Si-5Gr composite. In hyper-eutectic Al-Si alloys due to extremely fast cooling in spray forming sometimes crack produces and very high porosity is existent. Cooling of liquid Al-18Si-5Gr composite takes place during their solidification in the gas stream. Defect or pore occurred by the shrinkage of liquid composite during its solidification.

### *3.2. XRD*

Figure 4 shows the XRD spectra of spray formed Al-Si-Gr composite before and after FSP. These XRD spectrums clearly indicate the presence of only three phases in the spray preforms and FSPed samples. XRD of spray formed material indicates the presence of graphite in the composite. With the increase in Si content, the intensity of peaks of Si in XRD spectra increases. After FSP, the XRD spectrum is similar to their spray formed counterparts; this shows the absence of any chemical reaction during FSP.

### *3.3. Porosity*

Various process factors such as spray deposition distance between nozzle and substrate, the inner diameter of melt release tube, melt superheat and atomising pressure affect the porosity of the spray deposited Al-Si-Gr composite. There are numerous types of porosities present in the composites, namely porosity because of hydrogen evolution, shrinkage during solidification, interstitial, intersplat boundary and mechanically entrapped gas [14-15]. Porosity is detrimental because it can considerably reduce hardness strength, toughness, and other properties. Table 2 exhibits the theoretical density, actual density, and porosity of the composites. Theoretical density was calculated through ASTM B 328-96. We see that there is about a 70% decrement in porosity after FSP, this is due to the hot working nature and stirring action which causes the reduction in porosity of the spray formed sample. The forward motion of tool results in the closure of pores present in spray formed composite. The FSP's rotating tool generates frictional heat and stirs the composite. As a result, there is a removal of porosity of the Al-Si-Gr composite.

### *3.4. Hardness*

Table 3 shows the hardness of spray formed and FSPed composites. It can be seen from the table that hardness increases with the increase in the percentage of silicon content. There is a sharp increase in VHN after FSP on spray formed specimens. The hardness of the Al-Si-Gr composite increases with the increase in the percentage of silicon content; this increase in hardness is due to the rise of hard silicon phase. Due to severe plastic deformation, recrystallization occurs in stir zone, and grain refinement takes place. Grain refinement and reduction in porosity are the significant reasons behind the increase of hardness after FSP [16].

### *3.5 Tensile Tests*

Stress-strain curves (figure 5) display the mechanical characteristics of aluminium-silicon-graphite composites in a uni-axial tensile test. Several parameters influence the mechanical characteristics in the aluminium-silicon-graphite composites such as, chemical composition, solidification rate, inter-metallics, defects etc. The fracture behavior of composites is mainly governed by α-dendrites' plastic deformation and straining particles' elastically. As the composites are plastic deformed the brittle particle start to form micro-cracks in the aluminium-silicon eutectic areas and in the phase of primary silicon. These micro-cracks propagate until a critical volume of crack is reached. This propagation leads to multiple crack coalescence and final fracture occurs. The pores present leads to weakening of the Al-Si-Gr composite by decreasing the stress-bearing area and therefore reduces the maximum stress the composite can resist without failure. Because of this reason, spray formed materials have less strength. Reduction in porosity leads to increase in strength.

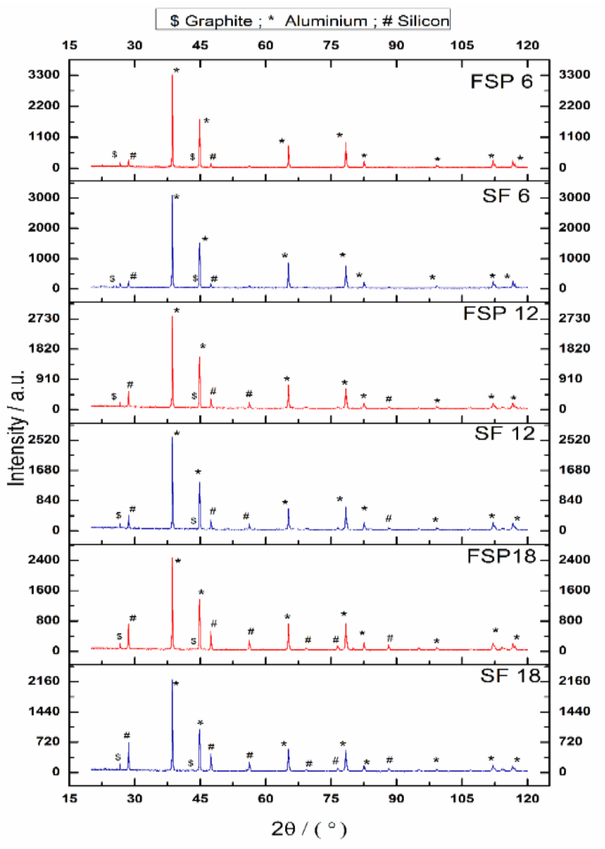


Figure 4. XRD Spectra of spray formed Al-Si-Gr composite before and after FSP

Figure 5 shows that there is continuous yielding in all composite compositions. Hence, no yield point can be determined. So, we calculate 0.2% proof stress. Mobile dislocations in aluminium are the reason behind continuous yielding behaviour. The shape, distribution, and size of eutectic and primary silicon particles determine the mechanical properties of the Al-Si-Gr composite. Strength properties of Al-Si-Gr composites are enhanced by spherical, small and uniformly distributed silicon particles [17]. Casting defects like porosity initiate cracks which lead to failure of aluminium-silicon alloys under tensile loading. These defects are reduced/eliminated by FSP resulting in improvement of mechanical properties.

Figure 5 shows the increase in ductility and UTS after FSP. Increase in tensile strength after FSP is due to refinement of microstructure [16], elimination of porosity and complete homogenisation of the microstructure attained after FSP. There is no significant change produced in yield point after FSP. This no substantial change in yield strength is produced because of the high yield strength of spray formed composite. Enhanced solidification of the molten composite on the spray deposited surface forms shallow shrinkage cavity which results in high yield strength of Al–Si-Gr composite. The aluminium matrix strength controlled the yield strength. Aluminium matrix strength depends on the microstructure of the formed composite (i.e., precipitate type and grain size). The increase in ductility after FSP can be attributed to the size reduction of Si phase particles in Al-matrix, complete homogenisation of composite and removal of porosity.

The variation in the stress-strain curve depends upon the silicon content, as shown in Figure 5. There is an increment in yield strength (YS) and ultimate tensile strength (UTS), but decrement in percentage elongation with the increase in Si content. Fine dimples present on the cracked surface represents the ductile fracture of all the samples. The decrease in percentage elongation with the increasing Si percentage in the composite may be attributed to the increasing fraction of Si-based phases which are plastically incompatible in the ductile and soft aluminium matrix. There is a slight decrement in the slope of the stress-strain curve with an increase in Si content. This slope represents Young's modulus. This shows a decrease in modulus of elasticity with an increase in Si content.

Table 3 shows the values of UTS, YS and percentage elongation for all compositions. The lower UTS of Al-18Si-5Gr composite can be mainly credited to the twin effects of the primary silicon and silicon-based phases which are plastically incompatible in the Al-matrix and increasing porosity. The presence of silicon in Al-matrix (plastically incompatible phases) causes stress to accumulate at the interface. During uniaxial tensile loading micro-voids/micro-cracks may emerge depending on the strengthening phase mechanical properties, thus decreasing UTS of the materials.

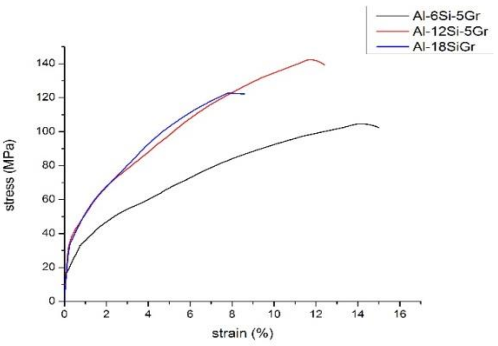


(a)

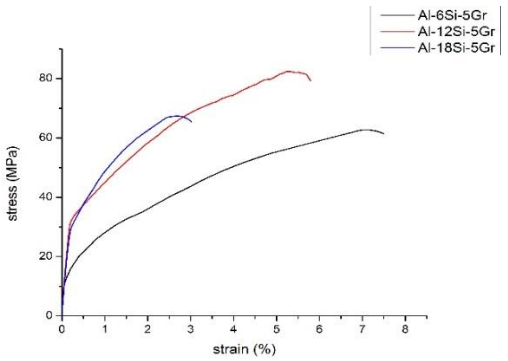


(b)

Figure 5. Stress-strain curves (a) Spray Formed (b) FSPed

## 4. Conclusions

1. The microstructure of spray formed Al-Si-Gr composite exhibits uniform dispersion of graphite particles throughout the matrix.
2. The coarse silicon particles present in spray formed composite become finer after FSP.
3. The small grain size of spray formed composite was further refined by FSP.
4. The hardness of composites increases with the increasing silicon content due to the rise of hard silicon phase; however, ductility reduced. Grain refinement and reduction in porosity are the significant reasons behind the increase of hardness after FSP.
6. The UTS, YS and percentage elongation of the composites are increased, but porosity decreased after FSP. There is a slight decrement in the slope of the stress-strain curve with an increase in Si content as silicon changes the nature of bonding in the composite.

## Acknowledgements

This work was supported by the Indian Institute of Technology, Roorkee, India.

## References

[1] F. Yu, D. S. Dwarakadasa, S. Ranganathan, Characterization of spray formed and cold rolled Al-Pb alloy, J Mater Process Technol 137 (2003) 164–167.

[2] P. S. Grant, Spray forming, Prog Mater Sci 39 (1995) 497–545.

[3] D. M. Goudara, K. Raju, V. C. Srivastava, G. B. Rudrakshid, Effect of secondary processing on the microstructure and wear behavior of spray formed Al–30Mg2Si–2Cu alloy, Mater Des 47 (2013) 489–496.

[4] K. V. Ojha, A. Tomar, D. Singh, G. C. Kaushal, Characterization of spray formed and cold rolled Al-Pb alloy, Mater Sci Eng A 487 (2008) 591–596.

[5] R. Mittal, D. Singh, Effect of Cold Rolling on the Mechanical Properties of Spray Cast Al-6Si-20Pb Alloy, Adv Mater Res 585 (2012) 402–406.

[6] R. S. Mishra, M. W. Mahoney, Friction Stir Processing: A New Grain Refinement Technique to Achieve High Strain Rate Superplasticity in Commercial Alloys, Mater Sci Forum, 357-359 (2001) 507–514.

[7] A. Hosseinzadeh, G. G. Yapici, High temperature characteristics of Al2024/SiC metal matrix composite fabricated by friction stir processing, Mater Sci Eng A, 731 (2018) 487–494.

[8] F. Khodabakhshi, B. Marzbanrad, L. H. Shah, H. Jahed, A. P. Gerlich, Friction-stir processing of a cold sprayed AA7075 coating layer on the AZ31B substrate: Structural homogeneity, microstructures and hardness, Surf Coat Technol 331 (2017) 116–128.

[9] D. Singh, S. Dangwal, Effects of process parameters on surface morphology of metal powders produced by free fall gas atomization, J Mater Sci 41 (2006) 3853–3860.

[10] B. Cantor, K. H. Baik, P. S. Grant, Development of microstructure in spray formed alloys, Prog Mater Sci 42 (1997) 373–392.

[11] V. C. Srivastava , R. K. Mandal, S. N. Ojha, K. Venkateswarlu, Microstructural modifications induced during spray deposition of Al–Si–Fe alloys and their mechanical properties, Mater Sci Eng A 471 (2007) 38–49.

[12] R. P. Underhill, P. S. Grant, B. Cantor, Microstructure of spray-formed Al alloy 2618, Mater Des 14 (1993) 45–47.

[13] Z. Y. Ma, S. R. Sharma, R. S. Mishra, Effect of friction stir processing on the microstructure of cast A356 aluminum, Mater Sci Eng A 433 (2006) 269–278.

[14] K. K. Sahu, R. K. Dube, S. C. Koria, Aspects of porosity formation in spray deposited thin aluminium strip, Powder Metall 52 (2009) 135–144.

[15] W. D. Cai, E. J. Lavernia, Modeling of porosity during spray forming, Mater Sci Eng A 226-228 (1997) 8–12.

[16] N. Hansen, Hall–Petch relation and boundary strengthening, Scripta Mater 51 (2004) 801–806.

[17] P. R. Guru, F. Khan MD, S. K. Panigrahi, G. D. Janki Ram, Enhancing strength, ductility and machinability of a Al–Si cast alloy by friction stir processing, J Manuf Process 18 (2015) 67–74.